Research article

SURFACE and INTERFACE ANALYSIS

Received: 20 December 2016 Revised: 16 February 2017 Accepted: 17 February 2017 Published online in Wiley Online Library: 22 March 2017

(wileyonlinelibrary.com) DOI 10.1002/sia.6227

Extracting the dielectric function from high-energy REELS measurements

Maarten Vos[a]* and Pedro L. Grande[b]

A method is described for extracting the dielectric function directly from a reflection electron energy loss spectrum taken at relatively high energies (2.5 to 40 keV). It makes simplifying assumptions on separation of surface and bulk losses. The approach uses a description based on partial intensities and surface excitation parameters and fits directly the reflection electron energy loss data. Several different model dielectric functions are implemented (extended Drude, Drude Lindhard, Mermin, and the Levine–Louie dielectric functions with relaxation time), and their advantages and disadvantages are discussed. Justification of this approach is in the end based on a comparison with the dielectric function as obtained by other means, which is generally quite good, provided that the solution obtained is restrained by sum rules to the right refractive index and electron density. The fitting program, to be used in conjunction with commercial plotting software, is provided.

Additional supporting information may be found in the online version of the publisher's web-site.

Keywords: reflection electron energy loss spectroscopy; dielectric function; aluminum; diamond; copper

Introduction

It has been known for a long time that electron energy loss measurements contain information about the dielectric function of a material.[1,2] In the case of (transmission) electron energy loss spectroscopy ((T)EELS), the measurements resemble, for thin enough samples, $\mathrm{Im}[\frac{-1}{\epsilon(\omega,q)}]$ with ϵ the dielectric function of the material under investigation, q the transferred momentum (selected by the detector angle), and ω the energy loss. $\mathrm{Im}[\frac{-1}{\epsilon(\omega,0)}]$ is often called the energy loss function (ELF).

For reflection electron energy loss spectroscopy (REELS), this relation is not so simple, as surface excitations, multiple bulk excitations, and elastic deflections from nuclei are all an integral part of the measurement. Nevertheless, there is a rich literature on this topic (see, e.g. References[3–8]) and it is clear that the main features of the dielectric function can be derived from REELS measurements.

For the analysis of the REELS spectra, which are a consequence of multiple interactions of the projectile with the target, one has to make simplifying assumptions. One such simplification is assuming a simple functional form for the dielectric function. For example, for free-electron materials like aluminum, the dielectric function can be parameterized as a Drude or Mermin loss function. Extracting the dielectric function simplifies then in the determination of the parameters of the model loss function. For more complicated materials (e.g. transition and noble metals), there is a richer structure of the loss spectrum, and a good description can only be obtained if a more complicated model (e.g. the sum of several simple loss functions) is used.

These model functions differ often dramatically in how they deal with dispersion, i.e. the dependence of the dielectric function on q. REELS, by its nature, samples $\mathrm{Im}[\frac{-1}{\epsilon(\omega,q)}]$ over a range of q values, but with increasing incoming energy E_0, the measurement gets skewed more and more towards small q values.

Dielectric functions are constrained by sum rules (Kramers–Kronig, F sum, Bethe sum, etc.).[9] If the dielectric function obtained by the fitting process does not obey these sum rules, then they are of very limited value.

Most approaches for extracting the dielectric function from a measurement rely on a two-step process. First, one or more single-scattering loss function(s) (either one mixed surface-bulk loss function[3,4] or a surface and a bulk loss function[6,7]) is extracted from the measurement. Then these derived distribution(s) is/are fitted with a dielectric function. Here, we will follow a different approach and fit the experimental spectrum directly.

In the process, some simplifying assumptions are made. Generally, these assumptions are less justified for lower incoming energies and/or more surface-sensitive geometries. The approach is thus most suitable for conditions where the surface loss excitation probability is relatively small.

At very high incoming energies, especially for light elements, there are complications due to recoil processes.[10] This sets a limit to the effective energy resolution one can obtain at very high incoming energies.

* *Correspondence to: Maarten Vos, Electronic Materials Engineering Department, Research School of Physics and Engineering, The Australian National University, Canberra 2601, Australia.*
E-mail: maarten.vos@anu.edu.au

a *Electronic Materials Engineering Department, Research School of Physics and Engineering, The Australian National University, Canberra 2601, Australia*

b *Ion Implantation Laboratory, Instituto de Física, Universidade Federal do Rio Grande do Sul, Av. Bento Goncalves, 9500, CP 15051, Porto Alegre, RS CEP 91501-970, Brazil*

Model dielectric functions

Away from a surface, the probability that an energetic electron loses a certain amount of energy, accompanied by a momentum transfer q, is proportional to the loss function:

$$\mathrm{Im}\left[\frac{-1}{\epsilon(\omega,q)}\right] = \frac{\epsilon_2(\omega,q)}{\epsilon_1(\omega,q)^2+\epsilon_2(\omega,q)^2} \quad (1)$$

with $\epsilon(\omega,q) = \epsilon_1(\omega,q) + i\epsilon_2(\omega,q)$ and ϵ_1, ϵ_2 real. Here, we give a brief overview of different model dielectric functions that can be used to model (R)EELS data. Other descriptions are given in, e.g. the books of Egerton[9] or Raether[11] or a recent review by Nikjoo *et al.*[12]

We describe first models of the dielectric function based on a semi-classical picture. In one such approach, the electrons are divided into free valence electrons and bound electrons. The dielectric function in this extended Drude model (Drude free-electron model extended with bound electrons) $\epsilon(\omega,q)$ is then given by

$$\epsilon_1(\omega,q) = \epsilon_b - \sum_i \frac{A_i(\omega^2-\omega_i(q)^2)}{(\omega^2-\omega_i(q)^2)^2+\Gamma_i^2\omega^2} \quad (2)$$

$$\epsilon_2(\omega,q) = \sum_i \frac{A_i\Gamma_i\omega}{(\omega^2-\omega_i(q)^2)^2+\Gamma_i^2\omega^2} \quad (3)$$

where A_i (in units of (energy)^2) relates to the density of electrons with binding energy ω_i. ω_i may depend on q. Γ_i determines the width of the excitation. ϵ_b is the background dielectric constant due to the polarizability of the core electrons.

Assuming all electrons are free ($\omega_i = 0, \epsilon_b = 1$), one obtains the Drude model. At $q = 0$, the corresponding dielectric function can be written as follows:

$$\epsilon(\omega,0) = \epsilon_1 + i\epsilon_2 = 1 - \frac{\omega_p^2}{\omega^2+\Gamma^2} + \frac{i\Gamma\omega_p^2}{\omega(\omega^2+\Gamma^2)} \quad (4)$$

with ω_p the plasmon energy $\omega_p = \sqrt{A_i} = \sqrt{\frac{Ne^2}{\epsilon_0 m}}$ with N the density of the electrons and m the electron mass. We will mainly use atomic units, then the relation between ω_p and N is simply $\omega_p^2 = 4\pi N$. In this case, the loss function can simply be expressed as follows:

$$\mathrm{Im}\left[\frac{-1}{\epsilon(\omega,q)}\right] = C\frac{\omega\Gamma\omega_p(0)^2}{(\omega^2-\omega_p(q)^2)^2+\omega^2\Gamma^2} \quad (5)$$

and for the real part:

$$\mathrm{Re}\left[\frac{1}{\epsilon(\omega,q)}\right] = 1 + C\frac{(\omega^2-\omega_p(q)^2)\omega_p(0)^2}{(\omega^2-\omega_p(q)^2)^2+\omega^2\Gamma^2} \quad (6)$$

with $C = 1$. Again, we allow for dispersion, i.e. the plasmon energy $\omega_p(q)$ can vary with q as will be discussed later. Using $C = 1$, we find $\mathrm{Re}\left[\frac{1}{\epsilon(0,0)}\right] = 0$, consistent with $\epsilon_1(0,0) = \infty$ as is the case for a metal. If we take $0 < C < 1$, then $0 < \mathrm{Re}\left[\frac{1}{\epsilon(0,0)}\right] < 1$ that corresponds to an insulator with refractive index n determined by $n^2 = \epsilon_1(0,0)$. In this way, the model can be used to describe an insulator.

Except for free-electron materials, such a dielectric function is a very poor approximation. One way forward is the electron gas statistical model as described, e.g. by Ritchie and Howie[13] and used by, e.g. Tung *et al.*[14] and Tougaard and Kraaer.[15] It is usually referred to as Drude–Lindhard model, as Lindhard added the q-dependence to the Drude model. It recognizes that the electron density $N(r)$ (and hence, ω_p) is not constant in a solid, but assumes that the response of the solid is equal to weighted sum of different solids with constant electron density. The weighting coefficient is proportional to the fraction of the solid with the corresponding density.

In a fitting procedure, one would approximate the continuously varying density $N(r)$ by a number of discrete densities N_i and corresponding plasmon frequency $\omega_i(q)$ that is often taken to depend on q as well. The corresponding loss function becomes then

$$\mathrm{Im}\left[\frac{-1}{\epsilon(\omega,q)}\right] = \sum_i C_i\frac{\omega\Gamma_i\omega_i(0)^2}{(\omega^2-\omega_i(q)^2)^2+\omega^2\Gamma_i^2} \quad (7)$$

and for the real part:

$$\mathrm{Re}\left[\frac{1}{\epsilon(\omega,q)}\right] = 1 + \sum_i C_i\frac{(\omega^2-\omega_i(q)^2)\omega_i(0)^2}{(\omega^2-\omega_i(q)^2)^2+\omega^2\Gamma^2} \quad (8)$$

with C_i the fraction of the volume for which the density is approximated such that the plasmon frequency is ω_i. Now, when $\sum_i C_i = 1$, the system is a metallic, and if $\sum_i C_i < 1$, the system is an insulator with the static refractive index n given by $1/n^2 = 1/\epsilon(0,0) = 1 - \sum_i C_i$. The fact that for insulators, $\sum_i C_i < 1$ means that, when interpreting the dielectric function along the lines of Ritchie and Howie,[13] one has to assume that part of the crystal has zero density of electrons, see Reference[16] for a more extensive discussion.

Alternatively, one can use Eqns (2) and (3) directly and try to describe the REELS measurements in that way. This method was used by, e.g. Werner *et al.* for metals[17] and Kwei *et al.* for insulators.[18] Now, it is not possible anymore to write the loss function in the relatively simple form of Eqn (5). Instead, we have to evaluate ϵ_1 from Eqn (2) and ϵ_2 from Eqn (3) and subsequently obtain the loss function using Eqn (1). Predicting where the peaks in the loss function will appear is now less straightforward, as the different levels interact. For a metal, a fraction of the electrons should have $\omega_i = 0$, whereas for insulators, these electrons should be absent.

Dielectric functions are subject to sum rules. One of them is the Kramers–Kronig sum rule:

$$1 - \mathrm{Re}\left[\frac{1}{\epsilon(\omega,q)}\right] = \frac{2}{\pi}\,\mathrm{P}\int_0^\infty \mathrm{Im}\left[\frac{-1}{\epsilon(\omega',q)}\right]\frac{\omega' d\omega'}{\omega'^2-\omega^2} \quad (9)$$

When evaluated for a metal at $\omega = 0, q = 0$ the right-hand side evaluates to 1, as then $\mathrm{Re}\left[\frac{1}{\epsilon(0,0)}\right] = 0$ (Eqn (6)). For insulators, $\epsilon_2(0,0) \approx 0$ and then $\mathrm{Re}\left[\frac{1}{\epsilon(0,0)}\right] = \epsilon_1/(\epsilon_1^2+\epsilon_2^2) \approx 1/\epsilon_1 = 1/n^2$. This sum rule, when evaluated at $\omega = 0$, is very sensitive to the behavior of $\epsilon(\omega,q)$ for small values of ω. If we use either expressions Eqns (2) and (3) or Eqns (7) and (8), then the Kramers–Kronig relation is always adhered to.

Other important sum rules are the F-sum rule:

$$\frac{1}{2\pi^2}\int_0^\omega \omega'\epsilon_2(\omega',q)d\omega' = N \quad (10)$$

with N the number of electrons per unit volume with binding energy well less than ω, and the Bethe sum rule:

$$\frac{1}{2\pi^2}\int_0^\omega \omega'\mathrm{Im}\left[\frac{-1}{\epsilon(\omega',q)}\right]d\omega' = N \quad (11)$$

Both are usually evaluated at $q = 0$. By multiplying N with the unit cell volume, we obtain the number of electrons per unit cell that contribute to the REELS spectrum.

When using any of these model dielectric functions, the ELF is never strictly zero. Thus, modeling an insulator always fails to some extent in the band gap region. The intensity in the gap can be reduced by increasing the number of oscillators (and decreasing their width), but this approach is not very practical. Another way to model an insulator is by multiplying the right-hand side of the model loss function (e.g. Eqn (7)) by a step function $\Theta(\omega - E_{gap})$ and hence zeroing Im $[-1/\epsilon(\omega, q)]$ in the band gap. This approach is followed in the QUASES package.[4,19] However, this severs the link between ϵ_1 and ϵ_2 and, e.g. for the Drude model, Eqn (4) does then not apply anymore. Instead, Re$[1/\epsilon]$ has then to be recovered from Im$[1/\epsilon]$ via a Kramers–Kronig relation similar to Eqn (9), from which ϵ_1 and ϵ_2 can then be calculated subsequently.

In the previous, we did not specify the q dependence of $\epsilon(\omega, q)$. In these semi-classical models, the effect of dispersion is usually taken into account by assuming that ω_i depends on q, e.g. by assuming simple quadratic dispersion:

$$\omega_i(q) = \omega_i(q = 0) + \alpha q^2/2m \tag{12}$$

where α is a constant between 1 (for free electrons in metals) and 0 (for deeper levels and insulators). A slightly better approach, consistent with plasmon dispersion at low q and free-electron-type dispersion at large q values, is the 'full dispersion equation':

$$\omega_i(q) = \sqrt{\omega_i(0)^2 + \frac{2}{3}E_f q^2 + \frac{q^4}{4}} \tag{13}$$

Here, E_f is the Fermi energy. In principle Γ_i can also depend on q (see, e.g. Emfietzoglou *et al.*[20]) but this is not implemented for these semi-classical models.

A quantum approach to calculating the dielectric function was introduced for a free-electron gas by Lindhard.[21] The result $\epsilon_L(\omega, q)$ consisted in a delta function (pole) (describing plasmon excitations) and a continuous part (describing electron-hole excitations). Mermin modified Lindhard's description, adding relaxation of the plasmon and giving it in this way a finite width in energy (Γ):[22]

$$\epsilon_M(\omega, q) = 1 + \frac{(1 + i\Gamma/\omega)(\epsilon_L(\omega + i\Gamma, q) - 1)}{1 + i\Gamma/\omega\,[\epsilon_l(\omega + i\Gamma, q) - 1]\,/\,[\epsilon_L(0, q) - 1]} \tag{14}$$

This also makes it more amenable for comparison with experiment. It turns out that at $q = 0$, the Mermin loss function coincides with Eqn (5) but it becomes much broader for larger q values. The Mermin loss function will give at any q the same value for the Bethe and F-sum rule.

Except for free-electron metals, a single Mermin loss function is not a good description of a REELS spectrum. For other materials, a sum of Mermin loss functions can be used, analog to Eqn (7). It turns out that this approach improves the description of stopping of ions in metals based on the dielectric function.[23] The dielec-

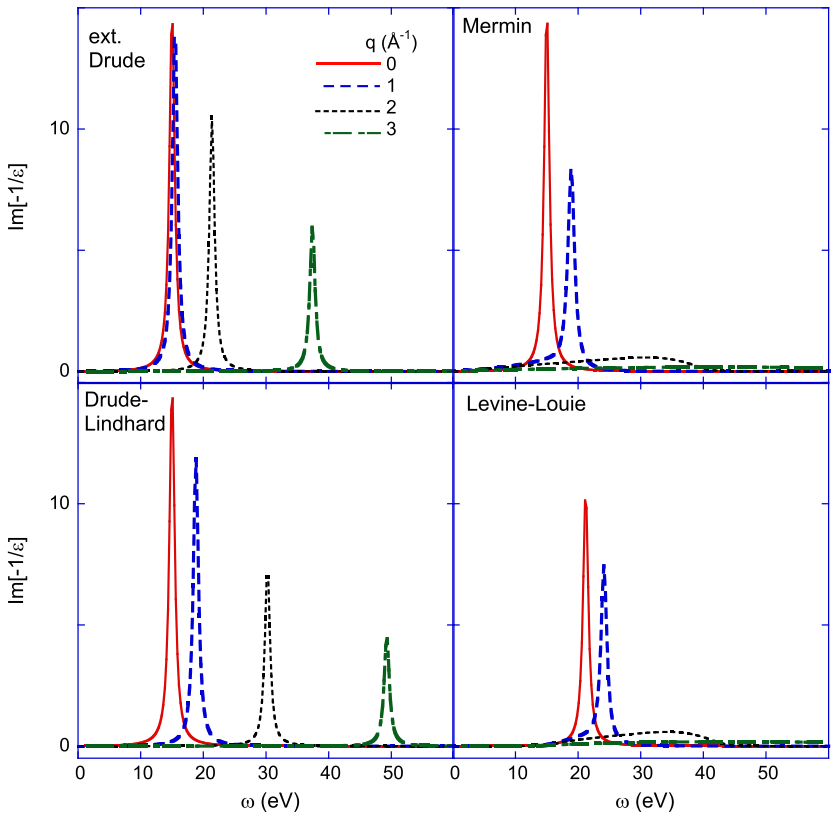

Figure 1. Examples of Im$[-1/\epsilon(\omega, q)]$ for the different models at the q values as indicated. Parameters used: extended Drude ($A = 225$ eV^2, $\omega = 0$ eV, $\Gamma = 1$ eV, and $\alpha = 1$), Drude–Lindhard ($A = 1$, $\omega = 15$ eV, $\Gamma = 1$ eV, and $\alpha = 1$), Mermin ($A = 1$, $\omega = 15$ eV, and $\Gamma = 1$ eV), and Mermin–Levine–Louie ($A = 1$, $\omega = 15$ eV, $\Gamma = 1$ eV, and U taken to be 15 eV). Note that for $q = 0$, the extended Drude, Drude–Lindhard, and Mermin models coincide. [Colour figure can be viewed at wileyonlinelibrary.com]

tric function based on a sum of Mermin oscillators can describe quite well both the optical limit and the high-momentum transfer (Compton) limit of the dielectric function.[24]

Levine and Louie (LL) proposed a variation on the Lindhard dielectric function suitable for insulators. In simple terms, they modified the imaginary part of $\epsilon_L(\omega, q)$ by transforming the energy axis according to $\omega'^2 = \omega^2 + U^2$ with U a quantity related to the band gap and calculated the corresponding real part via a Kramers–Kronig transformation.[25] The dielectric function obtained in this way $\epsilon_{LL}(\omega, q)$ is useful to describe insulators as it will result in finite static refractive index. Just as the Lindhard function the Levine–Louie loss function consist of a pole and a continuous part. Here, we propose that one can add relaxation (i.e. finite width to the pole) in the same way to the Levine–Louie function, as Mermin did to the Lindhard function, i.e. by replacing ϵ_L in Eqn (14) by ϵ_{LL}. It has the potential for describing the REELS spectrum of insulators, but, to our knowledge, its applicability has not been explored in the context of REELS. A disadvantage of the procedure sketched here is that after applying Eqn (14), the intensity of the loss function inside the band gap, although reduced, is not strictly 0.

The Levine–Louie and Mermin loss functions are mathematically more involved, and we refer for the explicit expression to the corresponding papers.[22,25] In our fitting program, we implemented extended Drude model (Eqns (2) and (3)), the Drude–Lindhard model (Eqns (7) and (8)), and the 'Mermin–Lindhard' (or just 'Mermin') loss function (Lindhard plus relaxation time) and the 'Mermin–Levine–Louie' (Levine–Louie plus relaxation time) models. Examples of the loss functions of these models at several q values are given in Fig. 1. As the

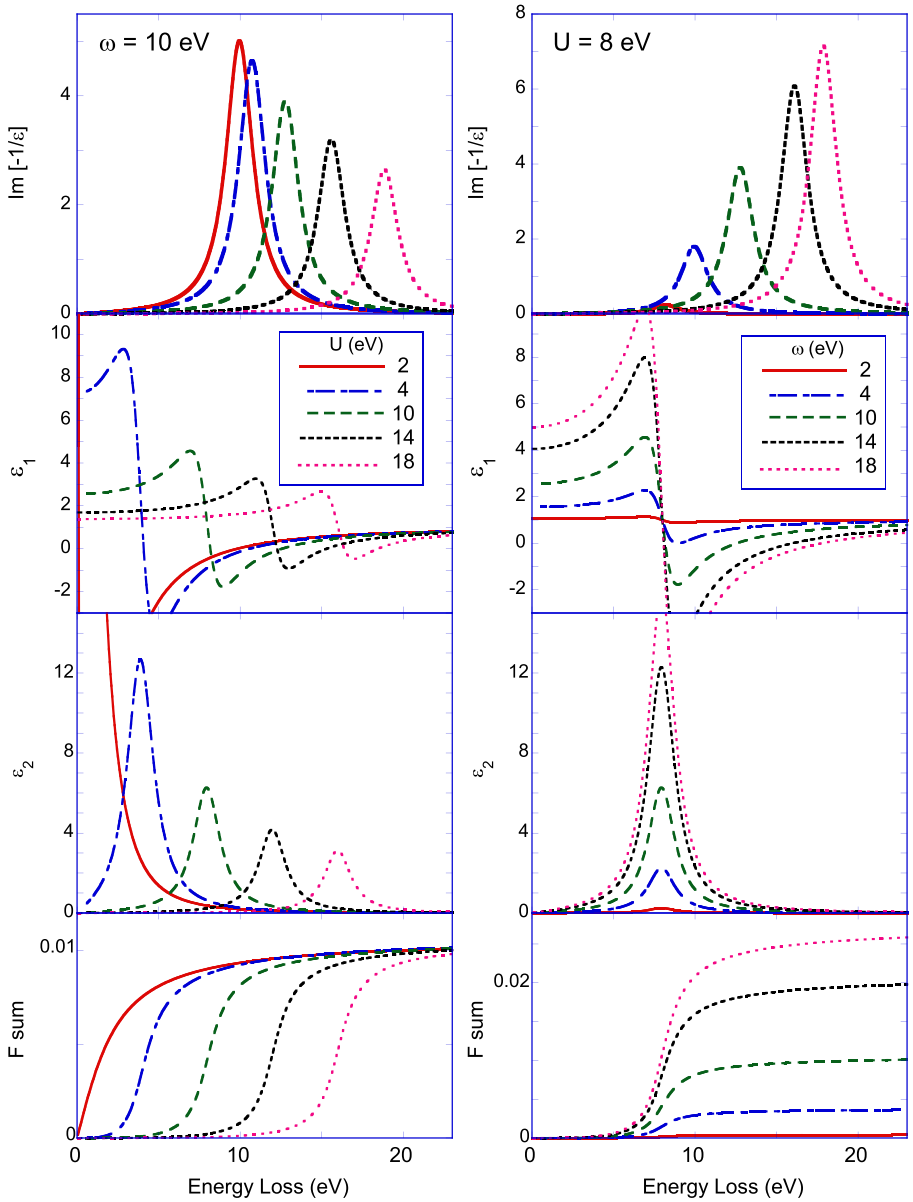

Figure 2. The top panels show the energy loss function for a single oscillator with $\omega = 10$ eV and $\gamma = 2$ eV for the 'Mermin–Levine–Louie' model for U values as indicated (thick lines) (left) and with $U = 8$ eV and $\gamma = 2$ eV for ω values as indicated (right). The central panels show the real and imaginary part of the corresponding dielectric function. The bottom panels show the development of the F-sum integral (Eqn (10)). [Colour figure can be viewed at wileyonlinelibrary.com]

Mermin–Levine–Louie model is not widely used, we show in Fig. 2 how the ELF, ϵ_1, ϵ_2, and the F-sum integral (Eqn (10)) develop as a function of U for a single oscillator with $\omega = 10$ eV and $\Gamma = 2$ eV and for $U = 10$ eV, $\Gamma = 2$ eV the dependence on ω.

Description of spectrum

In the approach used here, the loss spectrum is assumed to be due to bulk and surface excitations. The probability for bulk excitations is independent of the distance to the surface (i.e. 'begrenzung effects' are neglected) and is given by the differential inverse electron mean free path (DIIMFP) $W_b(\omega)$:

$$W_b(\omega, E_0) = \frac{1}{\pi E_0}\int_{q-}^{q+}\frac{dq}{q}\mathrm{Im}\left[\frac{-1}{\epsilon(\omega,q)}\right] \tag{15}$$

with $q_\pm = \sqrt{2E_0} \pm \sqrt{2(E_0-\omega)}$ and E_0 the incoming energy. W_b is the probability of energy loss ω per unit path length. This DIIMFP normalized to unit area (the NDIIMFP) is indicated by w_b.

The fitting procedure was written with relatively large kinetic energies in mind where the contribution of surface excitations is small and a fairly basic description of this quantity is probably good enough. The probability of surface excitations with energy loss ω is calculated for an electron impinging perpendicular to the surface as follows:[5]

$$P_s(\omega, E_0) = \frac{1}{\pi E_0}\int_{q-}^{q+}\mathrm{Im}\left[\frac{(\epsilon(\omega,q)-1)^2}{\epsilon(\omega,q)(\epsilon(\omega,q)+1}\right]\frac{|q_s|}{q^3}dq \tag{16}$$

with q_s the momentum component of along the surface. The use of Eqn (16) assumes that the electron was backscattered at a greater depth, than where the surface excitations occur. Then the simplifying assumption is made that for non-perpendicular trajectories, the surface excitation probability scales as $1/\cos\theta$ as suggested by Chen[26] and that the probability is the same for incoming and outgoing trajectories:

$$W_s(\omega, E_0) = P_s(\omega, E_0)(1/\cos\theta_1 + 1/\cos\theta_2) \tag{17}$$

with θ_1 and θ_2 the angle of the incoming and outgoing trajectory with respect to the surface normal. Again, w_s is the distribution W_s normalized to unit area. This is a very basic approach and could certainly be refined, see, e.g. the discussions in References.[27,28]

Without surface excitations, the REELS spectrum would be described as follows:

$$I_{\mathrm{bulk}} = c(I_0(\omega)+B_1 I_0 \otimes w_b(\omega)+B_2 I_0 \otimes w_b(\omega)\otimes w_b(\omega)+\ldots\ldots) \tag{18}$$

with c an overall scaling factor. For $I_0(\omega)$, we take the Gaussian that describes the elastic peak best. I_n is obtained by convoluting ($\otimes$) this Gaussian n–times with w_b. B_n is the contribution (partial intensity) of trajectories with n loss events relative to the elastic contribution. B_n is determined by the path length distribution, which depends on the angular dependence of the elastic scattering cross section, and can be retrieved in principle from Monte Carlo simulations. Note that by following this procedure, the resolution (both the resolution of the experiment and (especially at high energies) the Doppler broadening intrinsic to the sample) is included in I_0, and the bulk loss function w_b, for which the best fit with the experimental data is obtained, is not affected by the energy resolution.

In our approach, surface excitations are simply caused by an additional process. The average number of surface excitations is given by

$$\langle n_{\mathrm{surf}}\rangle = \int_0^\infty W_s(\omega, E_0)d\omega \tag{19}$$

We assume surface excitations follow a Poisson distribution, with p_0, p_1, and p_2 the probability of 0, 1, or 2 surface plasmons being created, then the actual observed spectrum can be calculated as follows:

$$I_{\mathrm{observed}} = p_0 I_{\mathrm{bulk}} + p_1 I_{\mathrm{bulk}} \otimes w_s + p_2 I_{\mathrm{bulk}} \otimes w_s \otimes w_s \tag{20}$$

The probability that more than two plasmons are created is assumed here to be negligible small.

Fitting procedure

In order to fit a spectrum, one assumes a dielectric function and a partial intensity distribution and calculated the REELS spectrum. Then, by comparison with the experiment, one adjusts either of these quantities, here performed in an automated way using a nonlinear fitting approach. However, there are some pitfalls that have to be avoided in order to obtain meaningful results.

In the fitting procedure, one wants to restrain the choice of dielectric function to those that are compatible with the static refractive index n and the electron density N (via the F or Bethe sum rule) of the material under investigation. When using the extended Drude model, one assumes a set of A_i values and checks if the F-sum rule is fulfilled:[18]

$$\sum_i A_i \stackrel{?}{=} 4\pi N \tag{21}$$

Generally, the F sum will not be adhered to. However, we can multiply all A_i values by a constant such that there is agreement with this sum rule. Note that, in the extended Drude model, the F sum does not depend on ω_i. As a consequence, if the F sum is fulfilled at $q = 0$, it will also be fulfilled at $q \neq 0$ even if ω depends on q.

Using the scaled A_i values, we now consider if ϵ_1 of Eqn (2) at $\omega = 0, q = 0$ corresponds to the right static refractive index:

$$\sum_i \frac{A_i}{(\omega_i(0)^2)} \stackrel{?}{=} n^2 - \epsilon_b = \epsilon_1(0,0) - \epsilon_b \tag{22}$$

Again, this generally will not be the case. We can, however, now multiply all oscillator energies ω_i by a constant such that the correct $n^2 - \epsilon_b$ value is obtained. For example, if the obtained value for $n^2 - \epsilon_b$ is twice too large, we multiple all ω_i values by $\sqrt{2}$. Note that this does not affect the F sum. Note also that this procedure only works if all ω_i, i.e. the material is not a metal.

In the fitting procedure, we start with an arbitrary set of oscillators. We rescale them first according to the earlier described procedure so that both the right refractive index and F-sum rule value are obtained and use this rescaled dielectric function to calculate the REELS spectrum, as described before (Eqn (20)). The fitting procedure determines then which dielectric function, that adheres to both sum rules, describe the spectrum best.

If this procedure is followed, not all A_i or ω_i are independent. This means that not all can be left as free parameters, at least one energy ω_i and one amplitude A_i has to be kept fixed. During the automated fitting procedure, the rescaling factors will vary, and hence, the ω_i and A_i parameters that are kept fixed will, after rescaling, vary as well.

For dielectric functions expressed in the Drude–Lindhard form, we have to modify the earlier procedure slightly. Now, we start by

rescaling the C_i values such that

$$\frac{1}{n^2} - 1 \stackrel{?}{=} \sum_i C_i \frac{(\omega^2 - \omega_i(q)^2)\omega_i(0)^2}{(\omega^2 - \omega_i(q)^2)^2 + \omega^2\Gamma_i^2} = -\sum_i C_i \qquad (23)$$

at $\omega = 0$ and $q = 0$. Note that this does not depend on ω_i. For a metal ($n = \infty$), this scaling assures that $\sum_i C_i = 1$. Using the rescaled C_i values, one could subsequently consider the F sum and try to rescale the ω_i values such that the right F-sum value is obtained. As the Drude–Lindhard dielectric function is expressed in terms of $\mathrm{Im}[-1/\epsilon(\omega, q)]$, it is more convenient to do this via the Bethe sum rule (Eqn (11)) that can be evaluated using $\int_0^\infty ax^2/\left[(x^2 - b^2)^2 + (ax)^2\right]dx = \pi/2$. The Bethe and F-sum rule are fulfilled if

$$\sum_i C_i\omega_i(0)^2 \stackrel{?}{=} 4\pi N \qquad (24)$$

Again, for an arbitrary set of ω_i values, this will generally not be the case, but we can multiply all energies ω_i by a constant such that the Bethe sum rule is adhered to. This rescaling will not affect the static refractive index. The Bethe sum rule depends on $\omega(0)$ not $\omega(q)$; thus, if the Bethe sum rule is adhered to at $q = 0$, it will be adhered to at all q values.

Similar to the Drude–Lindhard case (as at $q = 0$, the Mermin and Drude–Lindhard dielectric function coincide) for the Mermin loss function we can obtain a dielectric function that agrees with the Bethe sum rule if we rescale ω_i such that $4\pi N = \sum_i C_i\omega_i(0)^2$. As the Mermin loss function is intended to describe free-electron materials, $\sum_i C_i$ should be 1. See Reference[16] for the description of insulators using the Mermin loss function.

For the Mermin–Levine–Louie, we also always have $\sum C_i = 1$. We know that the F and Bethe sum is not affected by the U value, and for $U = 0$, the Mermin–Levine–Louie and Mermin loss function coincides. Hence, we start by scaling ω_i values such that the Bethe sum rule is adhered to, i.e. $\sum_i C_i\omega_i = 4\pi N$. Subsequently, U has to be manually adjusted until the right refractive index is obtained. An increase in U will lead to a decrease in n.

In practice, the dielectric function is only determined over a finite energy range. The density of electrons N obtained by the sum rules (Eqns (10) and (11)) is then approximately equal to the number of electrons with binding energy well less than the upper limit for which $\epsilon(\omega, q))$ was determined. For example, in the case of graphite or diamond, when the REELS data extending to 100-eV energy loss, the electron density is that of the valence electrons and the sum rule should approach four electrons per atom. For many other cases (e.g. transition metals) with shallow core

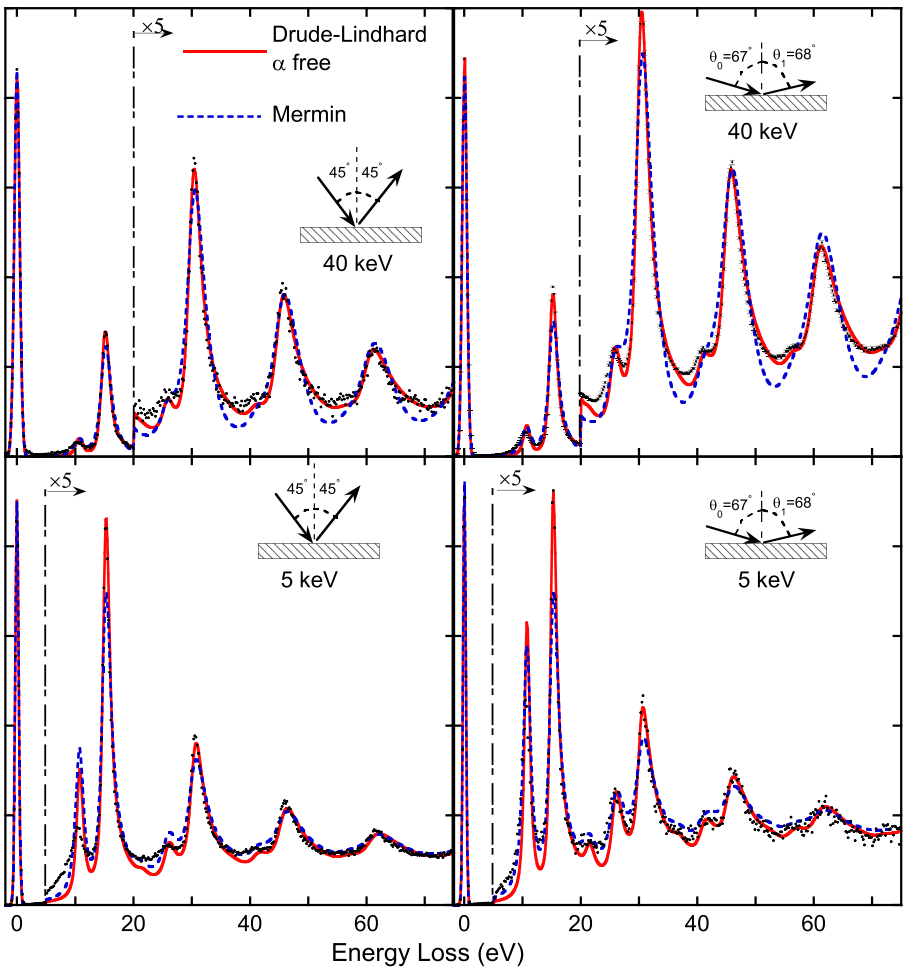

Figure 3. Fits of Al spectra taken at 40 and 5 keV for the different geometries shown. The dashed line is a fit based on the Mermin model. The fits based on the Drude–Lindhard model with $\alpha = 1$ are almost indistinguishable from the Mermin fits and are not shown. A better fit can be obtained using the Drude–Lindhard model with $\alpha = 2.3$ (solid line), but there is no obvious justification for such an α value. [Colour figure can be viewed at wileyonlinelibrary.com]

levels, it is often not straightforward to justify the expected value of the F and Bethe sum rule when the measurement only considers a finite energy loss range. This problem can be circumvented by assuming that for energies exceeding the measured range, the dielectric function is not affected by solid-state effects and can be described using their calculated atomic optical properties (e.g. using the tabulation from Reference[29]) beyond the range of the REELS measurement.[23]

Table 1. The various fitting parameters used for the fits of the diamond film spectra shown in Figs 4–6

Figure	A_i/C_i	γ_i (eV)	ω_i (eV)	U_i (eV)
4a	718, 58	11.9, 7.4	12.1, 29.4	—
4b	924, 43	12.5, 8.3	5.0, 29.7	—
4c	731, 56, 175	11.1, 6.4, 55	12.2, 28.9, 60	—
5, —	0.57, 0.38,0.045	11.5,8.5,82	25.2, 33.5,61	—
5, - - -	0.46, 0.28,0.09	12.0, 7.4,86	26.0, 33.7,61.5	—
6a	0.61, 0.39	11.9, 7.5	25.7, 33.2	5.4
6b	0.66, 0.34	13.2, 7.2	24.1, 31.6	12
6c	0.56, 0.35, 0.09	12, 7, 55	23.8, 31.5, 65	12

The parameter A_i has dimension eV^2 in the extended Drude model, and C_i in the other cases is dimensionless.
'—' represents thin solid line, and '- - -' represents thick dashed line.

A second group of input parameter is the partial intensities. If the energy loss region considered is 100 eV, then it will usually be enough to consider only the first 15 partial intensities. However, introducing 15 free parameters would never result in stable fitting outcomes. Instead, we use the fact that the partial intensities B_n are a smooth function of n. Because $B_0 = 1$, the following power series was used:

$$B_n = 1 + \sum_{i=1}^{i\text{max}} c_i n^i \tag{25}$$

In practice, a good fit of any partial intensity distribution obtained by Monte Carlo simulations can be obtained using terms up to $i_{\text{max}} = 3$. Thus, the partial intensity distribution can be modeled with three fitting parameters (c_1, c_2, and c_3).

There are some additional pitfalls to be taken care of. For a measurement performed only over a finite energy range, the DIIMFP will not be strictly zero outside this range. If a fraction y of the area extends beyond this range, then the NDIIMFP w_b should be normalized to $1 - y$, rather than 1. Even if y is small (say 0.05), then it still has a marked influence on the calculated spectrum, as the difference in normalization affects the nth convolution by a factor $(1 - y)^n$.

Another issue is the surface excitation probability. It is known to deviate from that calculated by Eqn (16), see, e.g. References.[30,31] When this is the case, the difference is, in first approximation, uniform, i.e. it differs by the same factor at all E_0 and $\theta_{1,2}$ values. It

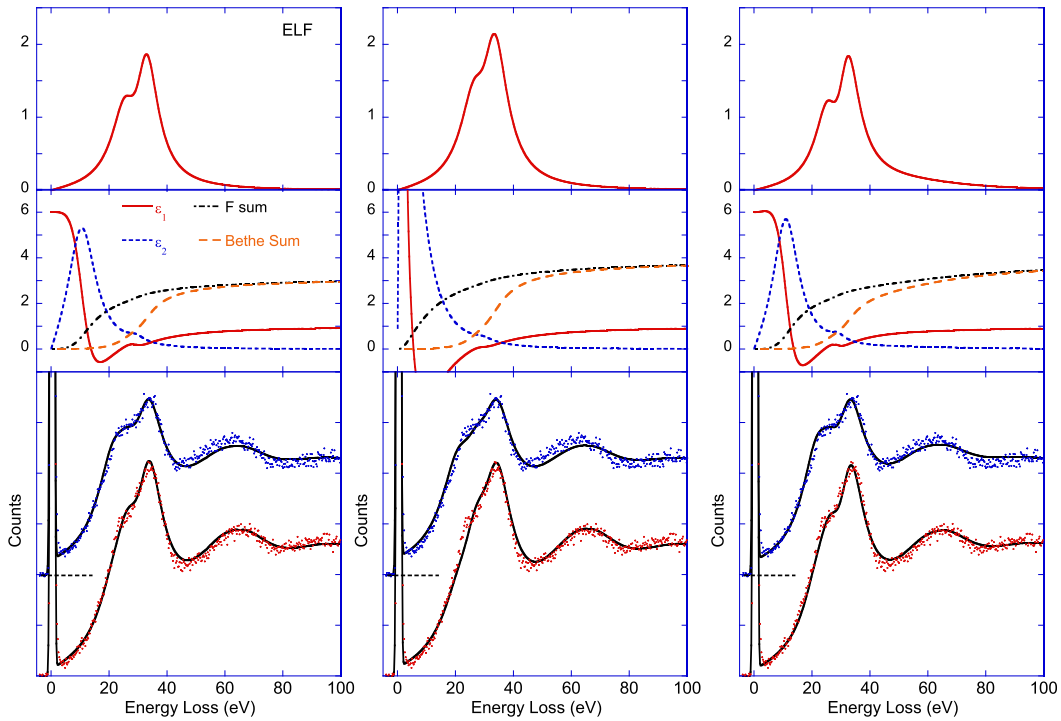

Figure 4. Examples of the analysis of the reflection electron energy loss spectroscopy data of a diamond film. The top panel shows the energy loss function (ELF) (Im$[-1/\epsilon]$) obtained by the fitting procedure. The panel below shows the corresponding ϵ_1 (solid line) ϵ_2 (short dash) as well as the results for the F (dash dot) and Bethe (long dash) sum rules integrated from zero to energy loss. The bottom panels show the raw data (dots) taken in a surface-sensitive (top, $\theta_0 = 35°$ and $\theta_1 = 80°$) and bulk-sensitive (bottom, $\theta_0 = 0°$ and $\theta_1 = 45°$) geometry and the fit itself. Both data sets were simultaneously fitted against a single model dielectric function using the extended Drude approach. In the left panel, two oscillators were used normalized such that the refractive index was reproduced. The center panel uses two oscillators and was normalized such that the F-sum rules was adhered to. The right panel uses an additional oscillator such that reasonable values are obtained for both the refractive index and F-sum rule. [Colour figure can be viewed at wileyonlinelibrary.com]

is thus often necessary to scale the calculated surface excitation parameter by a surface excitation adjustment factor. When more than one measurement is available, the same surface excitation adjustment factor is used for all of them.

In order to obtain stable results, it is required to have spectra available taken under different conditions extending up to at least 100-eV energy loss. In the following, we give some examples of the use of the program for some well-studied materials. The description is necessarily rather brief and should be seen as a first analysis of these cases, rather than their definitive treatment.

Results

Aluminum

The working of the procedure is best illustrated for the most simple case, and this is probably aluminum. This is not to say that the interpretation of the Al REELS spectrum in terms of its dielectric function is 100% complete. Yubero and Tougaard used a single Drude oscillator to describe their REELS measurements.[32] However, the width of this loss function did depend on the incoming electron energy, whereas the dielectric function of a material should describe REELS measurements taken at any energy. Pauly suggested that this could be explained by assuming that Γ depends on q, as the ranges of q values contributing to the spectrum (see the integration limits in Eqn (15)) changes with incoming electron energy.[33] Calliari *et al*. employed the Monte Carlo technique to compare measured energy loss spectra with theory.[34] They found less intensity for the first plasmon loss (relative to the elastic peak) in the simulation than observed in the experiment. Jiricek *et al*. noted that, in particular, higher-order plasmon peaks were more pronounced for single crystals than for polycrystalline samples.[35] This appears to indicate that the lattice has an influence on the loss spectrum and it should thus not be possible to describe it completely using a free-electron model.

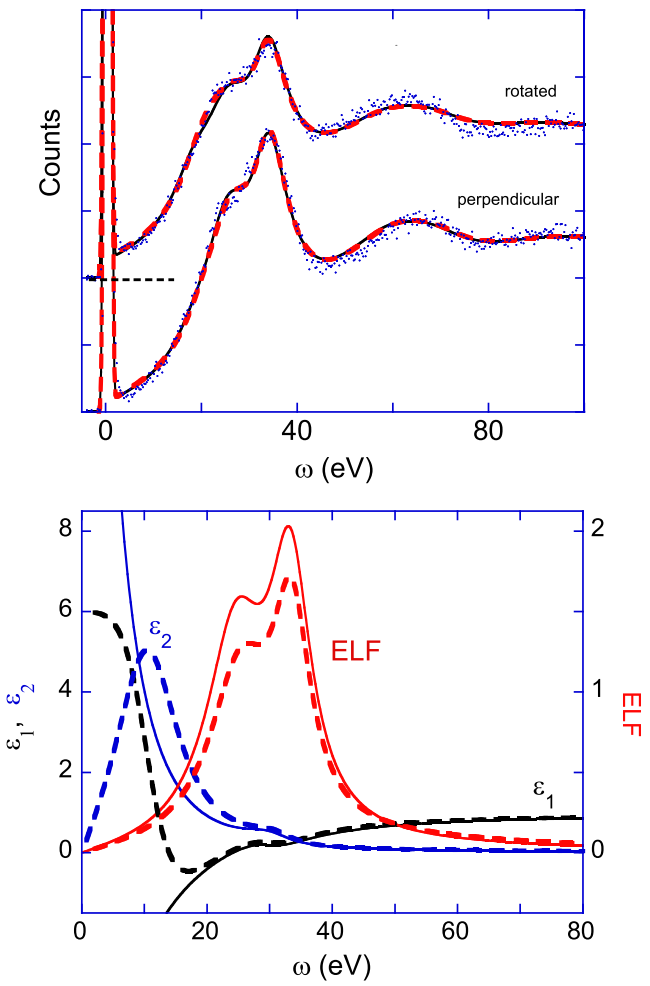

Figure 5. The same diamond film reflection electron energy loss spectroscopy spectra as shown in Fig. 4 but now fitted with Drude–Lindhard oscillators under the condition that $\sum_i C_i = 1$ (thin solid line) and $\sum_i C_i = 1 - 1/n^2$ (thick dashed line). The bottom panel shows the real and imaginary part and the energy loss function (ELF) of the corresponding dielectric functions. [Colour figure can be viewed at wileyonlinelibrary.com]

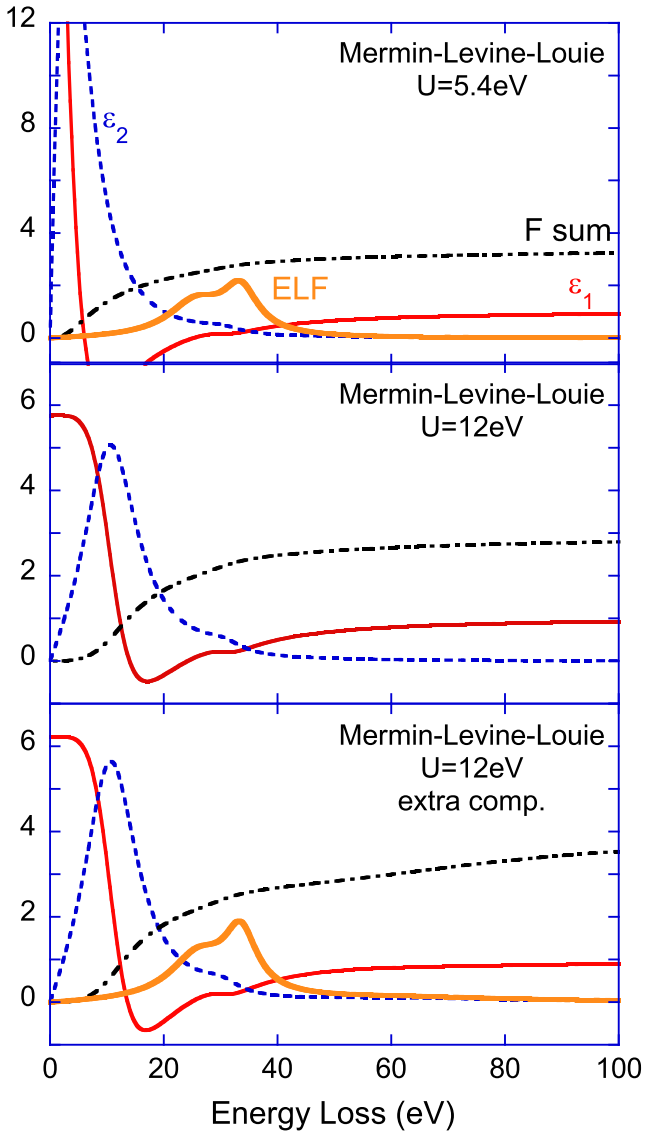

Figure 6. Real (ϵ_1) and imaginary (ϵ_2) part of the dielectric function as well as the energy loss function (ELF) and sum rule for the dielectric functions as indicated. In all cases, a reasonable fit of the experimental reflection electron energy loss spectroscopy data for the diamond film was obtained. [Colour figure can be viewed at wileyonlinelibrary.com]

We measured the aluminum plasmon peak at 5 and 40 keV in two different geometries. The results were fitted simultaneously with a single loss function (Drude–Lindhard oscillator) and a Mermin loss function, and the results are shown in Fig. 3. If one keeps the α parameter (Eqn (12)) of the Drude–Lindhard oscillator close to 1, the resulting fit is very close to the Mermin fit. These fits are not perfect as they have less intensity in between the plasmon peaks than experimentally observed. Within the Drude–Lindhard model, a better fit can be obtained by adjusting the α value to 2.3. However, there are no obvious justifications for such an α value. In transmission EELS work, the dispersion has been established experimentally, and no large enhancement relative to the simple picture described here was observed,[36,37] and the transmission results are in agreement with more detailed calculations.[38] The observed plasmon energy is quite close to the expected plasmon energy for a material with a free-electron density of aluminum. This means that the results are in agreement with the F and Bethe sum rules, assuming three electrons per atom.

Even with the α value adjusted in this way, the fit is not perfect. The observed surface plasmon is considerably wider in the experiment than in the calculation, as was observed as well by others.[32]

It should thus be emphasized that even for the most simple case of Al, the understanding of the REELS spectrum is far from complete. It is thus probably not justified to expect perfect descriptions for more complicated materials. In these cases, one employs usually more than one oscillator. By increasing the number of fitting parameters, the fit will obviously improve. The accuracy of the obtained dielectric function will most likely not depend on the accuracy of the fit, but on how accurate the model employed describes the underlying physics. Nevertheless, we will try to obtain the best fit of the experiment in the following and compare the obtained dielectric function with those derived using different approaches. The use of sum rules is essential to obtain meaningful dielectric functions, as will be illustrated next.

Diamond

The sample was a 2-μm thick diamond film grown on a Si wafer obtained from MTI corporation. Examples of the loss spectrum are shown in Fig. 4. We want to use this case to illustrate how the choice of fitting model affects the derived dielectric function and how sum rules can be used to obtain the best estimate of the parameters involved. For simplicity, we assume here that the refractive index and density of the diamond film is the same as that of bulk diamond.

Diamond is an insulator with a loss function that is usually described as consisting of a plasmon. In reality, the shape of the loss structure is not completely symmetric. The shoulder at the low-loss side only increases slightly if the sample is rotated to a surface-sensitive geometry. From this, we conclude that the shoulder is not exclusively due to surface plasmons. Waidmann *et al.*,[39] using transmission EELS, attributed this shoulder to interband transitions. For wideband insulators, Eqn (16) overestimates the surface excitation probability;[30] hence, in the fits, the calculated surface plasmon intensity was reduced by a factor of 5. The two diamond REELS spectra, taken with $E_0 = 5$ keV in a bulk, and surface-sensitive geometry were analyzed simultaneously. The deduced parameters are reproduced in Table 1.

We start with discussing a fitting approach based on the extended Drude model using two oscillators. First, the amplitude of the oscillators were restricted, using Eqn (22), such that the established refractive index was obtained. Good fits were obtained (Fig. 4a). However, the Bethe and F-sum rules resulted in only approximately three electrons per C atom, rather than the expected 4. Next, the fit was performed using Eqn (21) as a constrained such that the Bethe and F sum reproduce the correct electron density (Fig. 4b). This gave good fits as well. However, now, the value ϵ_1 at $\omega = 0$ was much too large ($\epsilon_1 \approx 38$) inconsistent with the static refractive index of diamond.

In order to obtain a good fit and agreement with both sum rules, a third component is required. There is no direct experimental justification in the measured REELS spectrum itself for this. However, by adjusting the partial intensities slightly, one can obtain an equally good fit assuming a broad third component at somewhat higher-loss values. The fit was performed under the constraint that both the right F-sum (and Bethe) rule and refractive index were obtained (Fig. 4c). As there are no clear features in the REELS spectrum associated with this third component, one can vary its parameters somewhat (position, width, and intensity) and obtain fitting results of similar quality.

Now, consider a fit using Drude–Lindhard oscillators. It is possible to obtain a good fit with the sum of the coefficients $\sum_i C_i = 1$ (Fig. 5). However, the obtained dielectric function reflects its free-electron origin and fails to reproduce the right refractive index as ϵ_1 assumes large negative values for $\omega \to 0$. (Fig. 5 lower panel). The same applies when using the Mermin loss function (again with $\sum_i C_i = 1$), which results in a virtually identical fit and dielectric function at $q = 0$. This is understandable as the dielectric function at higher q values, where the Mermin and Drude–Lindhard approaches differ greatly (Fig. 1) contribute only very little to the DIIMFP (Eqn (15), this is the case especially when E_0 is large). Thus, the Drude–Lindhard and Mermin approach with

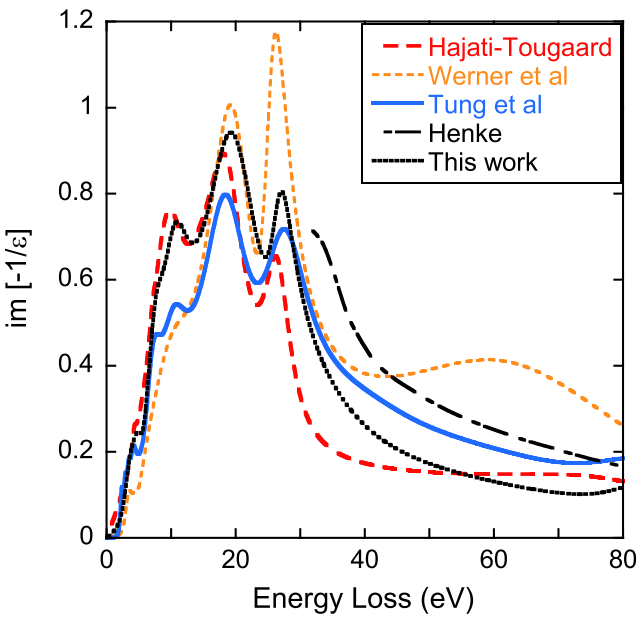

Figure 7. A comparison of the energy loss function of Cu as obtained from the dielectric function published by several authors. The energy loss function from Hajati and Tougaard[19] and the one obtained by Werner *et al.*[17] were obtained from reflection electron energy loss spectroscopy measurement. Tung *et al.* fitted optical data.[5] The one marked Henke is derived from atomic form factors.[29] [Colour figure can be viewed at wileyonlinelibrary.com]

$\sum_i C_i = 1$ do not fail in fitting the spectra, but fail to meet the additional boundary conditions.

As is described elsewhere,[16] a good agreement with the static refractive index n can be obtained, using the Drude–Lindhard model, if we take $\sum_i C_i = 1 - 1/n^2$. The corresponding ELF is slightly different but by adjusting the partial intensities slightly, it is again possible to obtain good fits. Now, the obtained dielectric function is not too different from the one obtained using the extended Drude approach or those reported in the literature for amorphous diamond films.[40] The dielectric function for crystalline diamond as derived from optical measurements has much more structure for energies below 15 eV.[41] Here, the intensity of the loss spectrum is very weak, and extracting these details (including the onset of the loss function, i.e. the band gap) is difficult experimentally.

As diamond is an insulator, it is attractive to try to describe it with a dielectric function derived from quantum mechanics that was intended for these materials. The Mermin–Levine–Louie dielectric function is thus more appropriate. Here, one has an additional parameter, U, that relates to the band gap. It was used as an adjustable parameter, but kept the same for all components of the fit. If we use a value of U that corresponds to the band gap (5.4 eV), then the value of ϵ_1 at $\omega = 0$ is still $\approx$4 times too large for the refractive index of diamond. The nominal refractive index was obtained using $U = 12$ eV, stressing that this parameter cannot be simply equated to the band gap. However, the F-sum value was

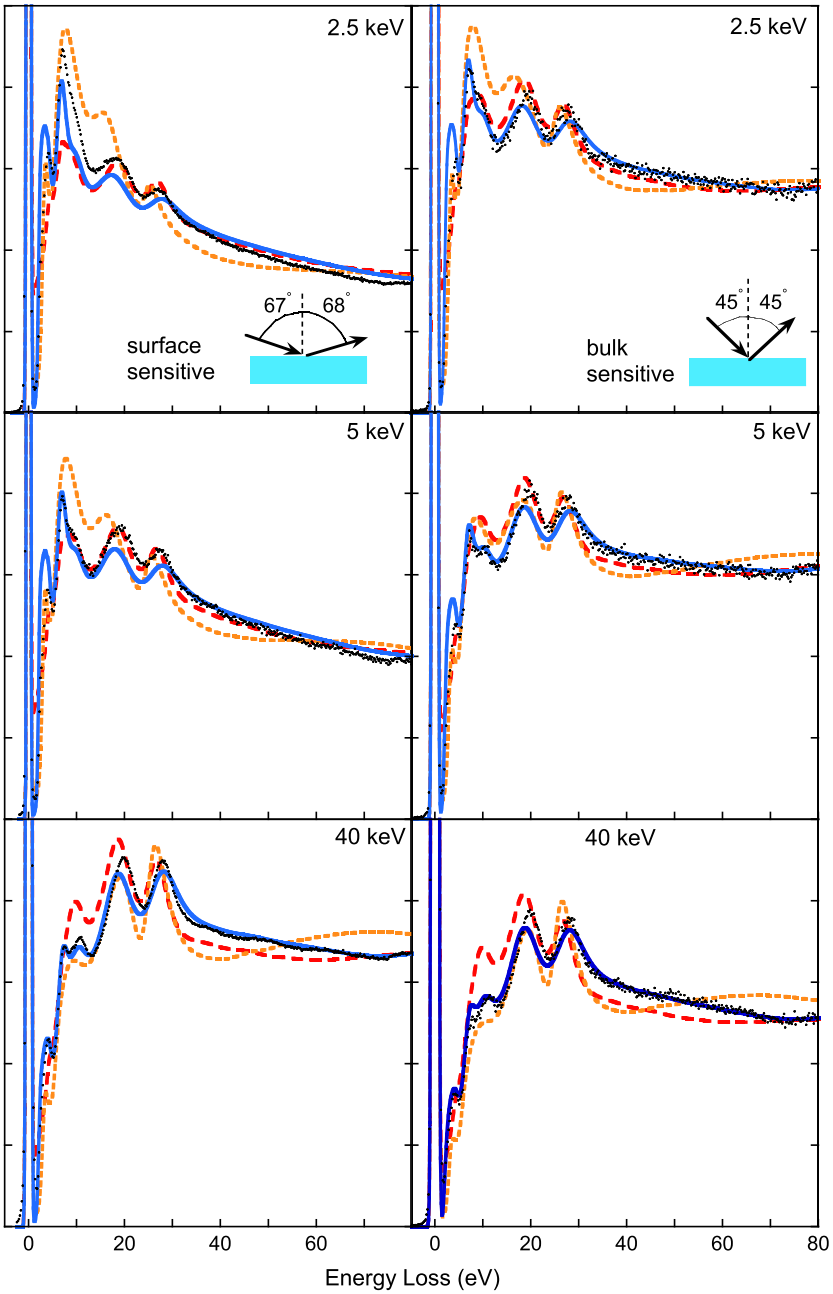

Figure 8. Fit of Cu reflection electron energy loss spectroscopy spectra (black dots) based on the dielectric function as published by Hajati and Tougaard (red dashed line)[19] Werner *et al.* (yellow dots)[17] and Tung *et al.* (solid blue line).[5] Data were taken in a surface-sensitive geometry (left) and a bulk-sensitive geometry (right) at energies as indicated. [Colour figure can be viewed at wileyonlinelibrary.com]

only ≈3 electrons per atom. Just as in the extended Drude case, a good fit with a better F-sum value can be obtained if a third, broad component was added, but the precise parameters for this third component are more difficult to obtain from this experiment. The results for this approach are given in the bottom panel of Fig. 6.

Table 2. The values for the SEA parameter obtained when fitted the present experimental data with the literature dielectric function

Method	SEA	c_1	c_2
Hajati	0.32	0.17, 0.14, −0.06	−0.05, −0.04, 0.02
Tung	0.53	0.28, 0.36, 0.56	−0.09, −.011, −.09
Werner	0.85	−0.06, 0.10, 0.46	−0.01, −0.05, −0.08
This work	0.54	−0.02,0.03, 0.24	−0.01, −0.02, −0.02

Also, given are the obtained coefficients c_1 and c_2 (Eqn (25)) for the glancing measurement at 2.5, 5, and 40 keV. c_3 was fixed at 0.
SEA, surface excitation adjustment.

The values used in all these fits are reproduced in Table 1. The partial intensities obtained from the fits were very close to 1, as expected for a low-*Z* target where the transport mean free path is very large.

When one compares all the dielectric functions obtained using the different models (Figs 4–6), then one sees that for $\omega > 20$, there is good agreement for ϵ_1 and ϵ_2. For $\omega < 20$, the differences are huge. All obtained ELFs have the same shape but slightly different amplitudes, except that their 'tails' are increased somewhat if a third component is added. Thus, one needs to have additional information about a sample (refractive index and density of valence electrons) for the dielectric function to be determined uniquely over the whole energy range.

Copper

Finally, we discuss the case of copper, as an example of a metal with a more complicated REELS spectrum. For Cu model, dielectric functions were published by Tung *et al.*[5] (based on optical measurements), Werner *et al.*,[17] and Hajati and Tougaard,[19] the latter

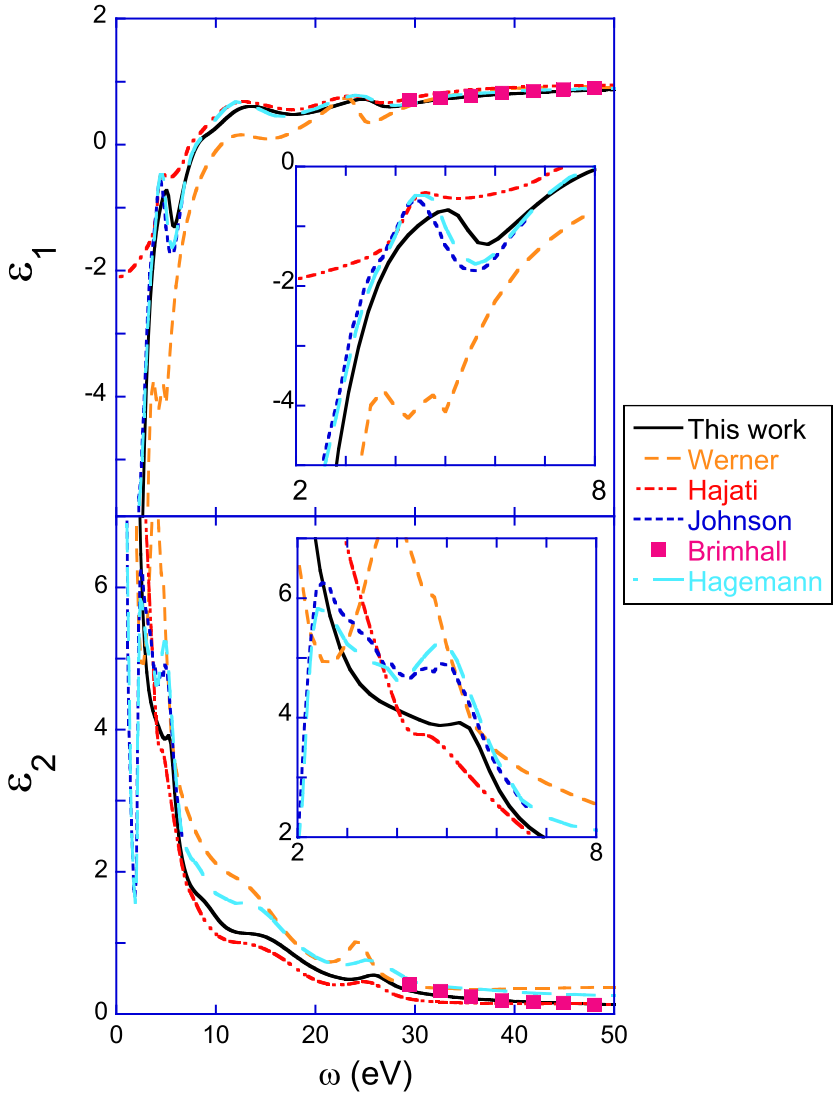

Figure 9. A comparison of the ϵ_1 and ϵ_2 as obtained here for Cu with values derived from reflection electron energy loss spectroscopy by Werner *et al.*,[17] Hajati *et al.*,[19] and by optical means by Johnson and Christy,[43] Brimhal *et al.*,[44] and Hagemann *et al.*[45] The insert shows the low-energy region on an expanded scale. [Colour figure can be viewed at wileyonlinelibrary.com]

two based on REELS measurements. The ELF of these dielectric functions are show in Fig. 7. There is another somewhat different set of parameters by Tahir and Tougaard,[42] but based on the same analysis method as Reference.[19] Unfortunately, there is considerable disagreement between the various ELFs. At larger ω values, it is expected that the dielectric function can be derived from atomic structure factors. Hence, we also show for energies above 30 eV the calculated loss function based on the Henke atomic scattering factors.[29]

Our measurement were performed for incoming energies between 2.5 and 40 keV and were taken either in a surface-sensitive glancing-in glancing-out geometry or a bulk-sensitive geometry. We now try to fit these data with the previously published model dielectric functions, using the partial intensities and the surface excitation adjustment factor as fitting parameters. The obtained values for the latter parameter varied from 0.85 when using the model function from Werner, 0.53 for the one of Tung *et al*., and 0.32 for the one of Hajati and Tougaard. The resulting fits are shown in Fig. 8. (The measurement and their fits extended up to 140-eV energy loss, but only the first 80 eV is shown in this figure. At higher-energy losses, no distinct structures are observed. This part of the spectra is, however, important in restraining the c_i parameters used to calculate the partial intensities used in the fits.) Clearly, one cannot obtain great fits for all dielectric function by only changing the partial intensities and the surface excitation adjustment factor. Examples of the values obtained are given in Table 2. Especially for the high-energy data, the dielectric function of Tung *et al*. describes our experimental data best. At high-energy losses, this function matches also best the loss function derived from Henke's atomic scattering factors.

Somewhat, better description of the experimental data is obtained if the dielectric function itself is fitted as well against the experimental data. The obtained ELF is shown in Fig. 7 as well, and the obtained real and imaginary part are compared in Fig. 9 with those obtained from other experiments. Agreement of our data is better with the dielectric function derived from optical data from Tung *et al*. than with those derived from lower-energy REELS data.

Discussion and conclusion

This work intended to make the extraction of the loss function from REELS measurements more transparent for either semi-classical or quantum-physics-based models of the loss function. Using quantum-physics-based dispersion models as present in Mermin and Levine–Louie dielectric function would be less *ad hoc*. However, at the energies employed here, dispersion affects the loss spectrum only in a very minor way, and virtually, the same results are obtained when using the Drude–Lindhard or extended Drude approaches. At much lower energies, this may not be the case, but then surface excitation and interference effect of the incoming and outgoing trajectories could require a more sophisticated modeling of these effects.[4,19,32]

For insulators, the use of model dielectric functions has the disadvantage that the intensity of the loss function is not truncated rigorously to zero in the band gap region but low-intensity tails exist. These tails affect, e.g. the Kramers–Kronig sum rule, as this quantity is very sensitive to the intensity of the loss function near zero loss. As a consequence, the value of ϵ_1 near $\omega = 0$ will be slightly too large.

The second motivation was to avoid the creation intermediate distribution (the effective loss function obtained with the Tougaard–Chorkendorff procedure or the DIIMFP and the DSEP as extracted from different spectra in the work of Werner *et al*.) and work straight from the experimental data. At least for energies above 2.5 keV, the direct approach has some clear advantages. For example, the chi-square of the fit is well defined as the statistical error bar is just the square root of the number of counts. The partial intensities obtained from the fit can be compared in principle to those obtained by Monte Carlo simulations, and discrepancies can be used to improve either the dielectric function or the Monte Carlo simulation procedure. This will be the focus of future work but especially for low-*Z* targets such as C and Al, the deviations from unity of the partial intensities are encouraging small.

Some papers (e.g. References[4,19,32]) deal with surface excitation and interference effects in a much more sophisticated way than is performed here. In these cases, the analysis is always performed starting with a single-scattering loss distribution obtained by the Tougaard–Chorkendorff procedure.[3] For the cases where there is a single sharp plasmon feature in the loss spectrum, it produces negative intensities for a certain energy loss range and is for those losses clearly not meaningful. The assumption that this single-scattering loss function has a well-defined meaning when it is always positive requires justification by comparing, e.g. the obtained dielectric function with optical data. From the comparison with the optical data for copper, it is not obvious that the Tougaard–Chorkendorff-based analysis, with sophisticated treatment of surface excitation and interference effects, results in a better estimate of the dielectric function, than the method described here.

The dielectric functions obtained are comparable with those published in the literature. In some cases (noble metals, only Cu was presented here), the agreement of the current dielectric function with those obtained by optical means is better than previous REELS studies. This is probably more due to the better energy resolution of the current spectrometer rather than the data analysis procedure followed.

In summary, we have demonstrated that the approach of extracting dielectric properties from a material by directly fitting the REELS data is at least competitive with more indirect approaches when applied to REELS at relatively high energies. We think that this method is a more transparent way of analysis and aid the discussion where interpretations of REELS experiments in terms of dielectric function differ.[46]

A basic manual of the fitting routine is provided as Supporting information. The source code of the DLL, to be used in conjunction with the Origin plotting program, can be obtained from the corresponding author.

Acknowledgements

The authors want to thank Mr G. Marmitt for testing the parts of the software. This work was made possible by a grant of the Australian Research Council. P. L. G. acknowledges funding from the Braziian agencies CNPq, INES, and FAPERGS.

References

[1] R. H. Ritchie, *Phys. Rev.* **1957**, *106*, 874–881.
[2] D. Pines, *Elementary Excitations in Solids*, Benjamin, New York, NY, **1963**.
[3] S. Tougaard, I. Chorkendorff, Differential inelastic electron scattering cross sections from experimental reflection electron-energy-loss spectra: application to background removal in electron spectroscopy, *Phys. Rev. B* **1987**, *35*, 6570–6577.

[4] F. Yubero, S. Tougaard, Quantitative analysis of reflection electron energy loss spectra, *Surf. Interface Anal.* **1992**, *19*, 269–273.
[5] C. Tung, Y. Chen, C. Kwei, T. Chou, Differential cross sections for plasmon excitations and reflected electron-energy-loss spectra, *Phys. Rev. B* **1994**, *49*, 16684–16693.
[6] W. S. M. Werner, Differential surface and volume excitation probability of medium-energy electrons in solids, *Phys. Rev. B* **2006**, *74*, 075421(1–14).
[7] W. S. M. Werner, *Surf. Sci.* **2010**, *604*, 290–299.
[8] B. Da, H. Shinotsuka, H. Yoshikawa, Z. J. Ding, S. Tanuma, *Phys. Rev. Lett.* **2014**, *113*, 063201.
[9] R. F. Egerton, *Electron Energy-loss Spectroscopy in the Electron Microscope*, Plenum Press, New York, **1996**.
[10] M. Vos, P. L. Grande, *Nucl. Instrum. Methods B* **2015**, *354*, 332–339.
[11] H. Raether, *Excitation of Plasmons and Interband Transitions by Electrons*, Springer tracts in modern physics; v.88, Springer Verlag, Berlin, **1979**.
[12] H. Nikjoo, D. Emfietzoglou, T. Liamsuwan, R. Taleei, D. Liljequist, S. Uehara, *Rep. Prog. Phys.* **2016**, *79*, 116601(1–55).
[13] R. H. Ritchie, A. Howie, *Philos. Mag.* **1977**, *36*, 463–481.
[14] C. J. Tung, J. C. Ashley, R. H. Ritchie, *Surf. Sci.* **1979**, *81*, 427–439.
[15] S. Tougaard, J. Kraaer, *Phys. Rev. B* **1991**, *43*, 1651–1661.
[16] M. Vos, P. L. Grande, *J. Phys. Chem. Solids.* **2017**, *104*, 192–197.
[17] W. S. M. Werner, K. Glantschnig, C. Ambrosch-Draxl, *J. Phys. Chem. Ref. Data* **2009**, *38*, 1013–1092.
[18] C. M. Kwei, Y. F. Chen, C. J. Tung, J. P. Wang, *Surf. Sci.* **1993**, *293*, 202–210.
[19] S. Hajati, O. Romanyuk, J. Zemek, S. Tougaard, *Phys. Rev. B* **2008**, *77*, 155403(1-11).
[20] D Emfietzoglou, F. Cucinotta, H Nikjoo, *Radiat. Res.* **2005**, *164*, 202–211.
[21] J. Lindhard, *K. Dan. Vidensk. Selsk. Mat.-Fys. Medd.* **1954**, *28*, no 8 1–57.
[22] N. Mermin, *Phys. Rev. B* **1970**, *1*, 2362–2363.
[23] I. Abril, R. Garcia-Molina, C. Denton, F. J. Pérez-Pérez, N. Arista, *Phys. Rev. A* **1998**, *58*, 357–366.
[24] M. Vos, *Nucl. Instrum. Methods B* **2015**, *366*, 6–12.
[25] Z. H. Levine, S. G. Louie, *Phys. Rev. B* **1982**, *25*, 6310–6316.
[26] Y. F. Chen, *Surf. Sci.* **2002**, *519*, 115–124.
[27] C. M. Kwei, Y. C. Li, C. J. Tung, *Surf. Sci.* **2006**, *600*, 3690–3694.
[28] B. Da, Y. Sun, S. F. Mao, Z. J. Ding, *Surf. Interface Anal.* **2012**, *45*, 773–780.
[29] B. L. Henke, E. M. Gullikson, J. C. Davis, *Atom. Data Nucl. Data Tables* **1993**, *54*, 181–342.
[30] N Pauly, M Novák, A Dubus, S Tougaard, *Surf. Interface Anal.* **2012**, *44*, 1147–1150.
[31] W. S. M. Werner, M. R. Went, M. Vos, *Surf. Sci.* **2007**, *601*, L109–L113.
[32] F. Yubero, S. Tougaard, *Phys. Rev. B* **1992**, *46*, 2486—2497.
[33] N. Pauly, A. Dubus, G. Monier, C. Robert-Goumet, M. A. Mahjoub, L. Bideux, B. Gruzza, *Surf. Interface Anal.* **2014**, *46*, 283–288.
[34] L. Calliari, M. Dapor, M. Filippi, *Surf. Sci.* **2007**, *601*, 2270–2276.
[35] P. Jiricek, I. Bartos, J. Zemek, W. S. M. Werner, *Surf. Sci.* **2010**, *604*, 1006.
[36] P. E. Batson, J. Silcox, *Phys. Rev. B* **1983**, *27*, 5224–5239.
[37] J. Sprösser-Prou, A. vom Felde, J. Fink, *Phys. Rev. B* **1989**, *40*, 5799–5801.
[38] K.-H. Lee, K. J. Chang, *Phys. Rev. B* **1994**, *49*, 2362–2367.
[39] S. Waidmann, M. Knupfer, B. Arnold, J. Fink, A. Fleszar, W. Hanke, *Phys. Rev. B* **2000**, *61*, 10149–10153.
[40] F. Xiong, Y. Y. Wang, R. P. H. Chang, *Phys. Rev. B* **1993**, *48*, 8016–8023.
[41] H. R. Phillip, E. A. Taft, *Phys. Rev.* **1964**, *136*, A1445–1448.
[42] D. Tahir, S. Tougaard, *J. Phys. Condens. Matter* **2012**, *24*, 175002–175002.
[43] P. B. Johnson, R. W. Christy, *Phys. Rev. B* **1972**, *6*, 4370–4379.
[44] N. Brimhall, N. Herrick, D. D. Allred, R. S. Turley, M. J. Ware, J. Peatross, *Opt. Express* **2009**, *17*, 23873–23879.
[45] H.-J. Hagemann, W. Gudat, C. Kunz, *J. Opt. Soc. Am.* **1975**, *65*, 742–744.
[46] M. Vos, P. L. Grande, *Surface Science* **2014**, *630*, 1–8.